

# MUTUAL INFORMATION BASED RATE ADAPTATION FOR MIMO-OFDM SYSTEMS WITH FINITE SIGNAL ALPHABETS

*Carsten Bockelmann, Dirk Wübben and Karl-Dirk Kammeyer*

University of Bremen

Department of Communications Engineering

{bockelmann, wuebben, kammeyer}@ant.uni-bremen.de

## ABSTRACT

We consider a single user MIMO-OFDM system where spatial multiplexing is applied and formulate rate allocation algorithms to adapt the used modulation alphabet on a per subcarrier basis. As a means to consider the system behavior including the channel code regarding bit or frame error rate (BER, FER) versus normalized average mutual information (NAMI) of an OFDM symbol for several  $M$ -QAM alphabets is investigated. To this end an approximation to the mutual information of MIMO systems with  $M$ -QAM signal alphabets is derived and compared to channel decomposition approaches to find a complexity/accuracy trade-off. Based on the mutual information results two algorithms using this channel knowledge are introduced. On the one hand, the error rates can be optimized assuming a fixed rate requirement and on the other hand the achieved transmission rate can be optimized under a BER/FER constraint. In both cases a NAMI threshold derived from the simulated system behavior for a specific channel code is used to adapt the allocated modulation alphabets via a greedy algorithm to achieve the target NAMI within an error margin.

## 1. INTRODUCTION

Adaptive communications for Orthogonal Frequency Division Multiple (OFDM) systems have been studied extensively, but mostly limited to the uncoded case, where the uncoded bit error rate (BER) is an often used target measure (e.g. [1],[2]). Practical coding typically has been neglected, but recently Ibi et. al [3] introduced a scheme based on the adaptation of the bit level channel coding with a fixed modulation size via Extrinsic Information Transfer (EXIT) charts for a frequency selective system with Minimum Mean Square Error (MMSE) turbo equalization. Obviously, this approach is limited by the chosen modulation alphabet, whereas Sankar et. al [4] and Li et. al [5] introduced algorithms to optimize the signal alphabets and transmission power over a set of orthogonal Gaussian channels if Low Density Parity Check (LDPC)

codes are applied. In both cases bit allocations have been optimized under the assumption of a fixed channel code. They showed mutual information (MI) to be a good optimization criterion for LDPC codes with regard to the error rate after decoding. Furthermore, results from Brueninghaus et. al [6] indicate that mutual information is an appropriate measure of channel quality to predict error rates reasonably well for convolutional and turbo codes. However, the calculation of the mutual information with finite symbol alphabets can only be solved numerically, which necessitates usable approximations. Especially, if multiple antennas are considered and linear precoding via an adequate decomposition of the channel is not applicable, e.g. for a low feedback scenario, numerical calculation becomes unfeasible (e.g. [7],[8]). Monte Carlo integration methods are one approach to this problem [9], but computational effort still remains high. To this end an approximation of the mutual information based on Jensen's inequality will be introduced in this paper, which allows the evaluation of the mutual information of Multiple Input Multiple Output (MIMO) channels without the need for numerical integration. Based on this approximation we propose two applications. First, a rate allocation scheme to enhance the bit error rate performance of coded MIMO-OFDM systems with a rate constraint and secondly a rate maximization scheme to optimize the number of transmitted bits under the constraint of a target error rate.

The remainder of the paper is organized as follows. In Section 2 the complex baseband system model is introduced. Afterwards an approximation to the mutual information of MIMO channels with finite symbol alphabets will be introduced in Section 3 and in Section 4 the Sorted QR Decomposition (SQRD) will be shown to simplify the calculations of this approximation. Then, in Section 4.3 an approach to allocate modulation alphabets to subcarriers of an OFDM symbol via the discussed mutual information approximation will be discussed. Two cases will be distinguished, rate allocation with a fixed BER/FER constraint and BER/FER enhancement with a fixed rate. In Section 6 simulation results will be presented and, finally, Section 7 will summarize the results.

---

This work was supported in part by the German Research Foundation (DFG) under grant Ka841-18.

## Notation

In the following, vectors and matrices are denoted by lower case and capital bold faced letters, respectively. We use  $(\cdot)^T$  for the matrix transpose and  $(\cdot)^H$  for conjugate transpose. The identity matrix of dimension  $n$  is denoted by  $\mathbf{I}_n$ .  $\mathbb{E}_{\mathbf{y}}\{\cdot\}$  denotes the expectation with respect to random variable  $\mathbf{y}$  and  $\mathcal{N}_C(\boldsymbol{\mu}, \boldsymbol{\Phi})$  describes a complex Gauss distribution with mean vector  $\boldsymbol{\mu}$  and covariance matrix  $\boldsymbol{\Phi}$ .

## 2. SYSTEM MODEL

The equivalent baseband system model of a MIMO-OFDM system with  $N_T$  transmit and  $N_R$  receive antennas in the frequency domain for subcarrier  $k = 1, \dots, N_C$  is given by

$$\mathbf{y}_k = \mathbf{H}_k \mathbf{x}_k + \mathbf{n}_k, \quad (1)$$

where  $\mathbf{y}_k \in \mathbb{C}^{N_R \times 1}$ ,  $\mathbf{x}_k \in \mathbb{C}^{N_T \times 1}$  and  $\mathbf{H}_k \in \mathbb{C}^{N_R \times N_T}$  denote the receive vector, transmit vector and channel matrix, respectively. Furthermore, the noise vector  $\mathbf{n}_k \in \mathbb{C}^{N_R \times 1}$  is complex Gaussian with  $\mathbf{n}_k \sim \mathcal{N}_C(\mathbf{0}, \sigma_n^2 \mathbf{I}_{N_R})$ .

The transmit vector  $\mathbf{x}_k$  is constructed as a function of the symbol vector  $\mathbf{d}_k \in \mathcal{A}^{N_T \times 1}$ , i.e.,  $\mathbf{x}_k = f(\mathbf{d}_k)$ , where  $\mathcal{A}$  denotes a set of symbols with cardinality  $M = |\mathcal{A}|$  (i.e.  $M$ -QAM). In the following we will restrict to the case of Spatial Multiplexing (SM) with variable alphabets  $\mathcal{A}_k$  per subcarrier. Throughout this paper equal power distribution in space and frequency is assumed, leading to

$$\mathbf{x}_k = \sqrt{\frac{\mathcal{P}}{N_T}} \mathbf{d}_k, \quad (2)$$

where  $\mathcal{P}$  denotes the transmit power per subcarrier. The channel matrix in frequency domain  $\mathbf{H}_k$  results from the  $N_C$ -point DFT of the frequency selective time domain channel  $\mathbf{H}(\ell) \in \mathbb{C}^{N_R \times N_T}$  with  $L_F$  taps. The elements of  $\mathbf{H}(\ell)$  are i.i.d. complex Gaussian distributed with  $\sigma_h^2 = 1$ .

The channel is assumed to be constant over one OFDM symbol, but changing independently between OFDM symbols. Exemplarily, two channel codes will be analyzed in this paper. On the one hand the  $[7, 5]_{\text{oct}}$  convolutional code (CC) and on the other hand the punctured half rate 3GPP Turbo Code (TC) [10]. Coding is applied to encode the data over one OFDM symbol only leading to varying code word lengths. In case of the turbo code  $N_{\text{ic}} = 8$  decoder iterations will be applied.

## 3. MUTUAL INFORMATION

Throughout Section 3 and 4 we will assume a deterministic MIMO channel (e.g. a realization of  $\mathbf{H}_k$ ). The mutual information of the communication system (1) disregarding the subcarrier index  $k$  for ease of notation is then well known to be [11]

$$h(\mathbf{x}; \mathbf{y}) = h(\mathbf{y}) - h(\mathbf{n}), \quad (3)$$

where  $h(\mathbf{y})$  denotes the entropy of the receive vector  $\mathbf{y}$  and  $h(\mathbf{n}) = N_R \log_2(\pi e \sigma_n^2)$  the entropy of the noise. The differential entropy  $h(\mathbf{y})$  is defined as

$$\begin{aligned} h(\mathbf{y}) &= \mathbb{E}_{\mathbf{y}}\{-\log_2(p(\mathbf{y}))\} \\ &= - \int_{\mathbb{C}^{N_R}} p(\mathbf{y}) \log_2(p(\mathbf{y})) d\mathbf{y}, \end{aligned} \quad (4)$$

where the probability density function  $p(\mathbf{y})$  can be expressed as

$$p(\mathbf{y}) = \sum_{\mathbf{x} \in \mathcal{X}} p(\mathbf{y}|\mathbf{x}) p(\mathbf{x}). \quad (5)$$

For each transmit vector  $\mathbf{x}$ , where  $\mathcal{X}$  is  $\mathcal{A}^{N_T \times 1}$  scaled with  $\sqrt{\mathcal{P}/N_T}$ , the marginal probability depends on the number of transmit symbols per layer

$$p(\mathbf{x}) = \frac{1}{M^{N_T}}, \quad (6)$$

whereas the probability of  $\mathbf{y}$  conditioned on  $\mathbf{x}$  under the assumption of white Gaussian noise results in

$$p(\mathbf{y}|\mathbf{x}) = \frac{1}{(\pi \sigma_n^2)^{N_R}} e^{-\frac{\|\mathbf{y} - \mathbf{H}\mathbf{x}\|^2}{\sigma_n^2}}. \quad (7)$$

### 3.1. Jensen's Inequality

Jensen's inequality is a well known way to lower bound expressions like (4) (and generally convex function)[11]

$$\mathbb{E}_{\mathbf{y}}\{-\log_2(p(\mathbf{y}))\} \geq -\log_2(\mathbb{E}_{\mathbf{y}}\{p(\mathbf{y})\}), \quad (8)$$

which leads to a much simpler formulation

$$\begin{aligned} h(\mathbf{y}) &\geq -\log_2 \left( \int_{\mathbb{C}^{N_R}} p(\mathbf{y}) p(\mathbf{y}) d\mathbf{y} \right) \\ &= -\log_2 \left( \int_{\mathbb{C}^{N_R}} p(\mathbf{y})^2 d\mathbf{y} \right). \end{aligned} \quad (9)$$

Inserting (6) and (7) in (5) leads to (10) considering the second line of (9), where the remaining integral  $\Theta$  can be solved in closed form. In order to illuminate this, it is useful to rewrite the arguments of the exponential functions.

$$\|\mathbf{y} - \mathbf{H}\mathbf{x}\|^2 = |y_1 - \mathbf{h}_1^T \mathbf{x}|^2 + \dots + |y_{N_R} - \mathbf{h}_{N_R}^T \mathbf{x}|^2, \quad (11)$$

with  $\mathbf{h}_i^T$  being the  $i$ th row of the channel matrix  $\mathbf{H}$ . Grouping terms stemming from  $\mathbf{x}_i$  and  $\mathbf{x}_\kappa$  with regard to the elements of  $\mathbf{y}$  leads to a product of independent integrals

$$\begin{aligned} \Theta &= \int_{\mathbb{C}} e^{-\frac{|y_1 - \mathbf{h}_1^T \mathbf{x}_i|^2 - |y_1 - \mathbf{h}_1^T \mathbf{x}_\kappa|^2}{\sigma_n^2}} dy_1 \dots \\ &\quad \int_{\mathbb{C}} e^{-\frac{|y_{N_R} - \mathbf{h}_{N_R}^T \mathbf{x}_i|^2 - |y_{N_R} - \mathbf{h}_{N_R}^T \mathbf{x}_\kappa|^2}{\sigma_n^2}} dy_{N_R}, \end{aligned} \quad (12)$$

$$\begin{aligned}
h(\mathbf{y}) &\geq -\log_2 \left( \int_{\mathbb{C}^{N_R}} \left( \sum_{\mathbf{x} \in \mathcal{X}} \frac{1}{(\pi\sigma_n^2)^{N_R} M^{N_T}} e^{-\frac{\|\mathbf{y}-\mathbf{H}\mathbf{x}\|^2}{\sigma_n^2}} \right)^2 d\mathbf{y} \right) \\
&= -\log_2 \left( \frac{1}{(\pi\sigma_n^2)^{2N_R} M^{2N_T}} \sum_{\mathbf{x}_i \in \mathcal{X}} \sum_{\mathbf{x}_\kappa \in \mathcal{X}} \underbrace{\int_{\mathbb{C}^{N_R}} e^{-\frac{\|\mathbf{y}-\mathbf{H}\mathbf{x}_i\|^2}{\sigma_n^2}} e^{-\frac{\|\mathbf{y}-\mathbf{H}\mathbf{x}_\kappa\|^2}{\sigma_n^2}} d\mathbf{y}}_{\Theta} \right), \tag{10}
\end{aligned}$$

where each integral can be solved in closed form

$$\begin{aligned}
&\int_{\mathbb{C}} e^{-\frac{|y_\rho - \mathbf{h}_\rho \mathbf{x}_i|^2 - |y_\rho - \mathbf{h}_\rho \mathbf{x}_\kappa|^2}{\sigma_n^2}} dy_\rho = \\
&\frac{1}{2} \pi e^{-\frac{1}{2\sigma_n^2} (|\mathbf{h}_\rho^T \mathbf{x}_i|^2 + |\mathbf{h}_\rho^T \mathbf{x}_\kappa|^2) - (\mathbf{h}_\rho^T \mathbf{x}_i^* \mathbf{h}_\rho^T \mathbf{x}_\kappa + \mathbf{h}_\rho^T \mathbf{x}_i \mathbf{h}_\rho^T \mathbf{x}_\kappa^*)} \forall \rho \tag{13}
\end{aligned}$$

This finally leads to

$$\Theta = \left( \frac{\pi}{2} \right)^{N_R} e^{-\frac{1}{2\sigma_n^2} (\mathbf{x}_i - \mathbf{x}_\kappa)^H \mathbf{H}^H \mathbf{H} (\mathbf{x}_i - \mathbf{x}_\kappa)}. \tag{14}$$

Using (14) in (10) and the abbreviation  $\Delta_{\mathbf{x}} = \mathbf{x}_i - \mathbf{x}_\kappa$  we achieve the loose lower bound

$$h(\mathbf{y}) \geq \underbrace{-\log_2 \left( \frac{\sum_{\Delta_{\mathbf{x}} \in \mathcal{D}} e^{-\frac{1}{2\sigma_n^2} \Delta_{\mathbf{x}}^H \mathbf{H}^H \mathbf{H} \Delta_{\mathbf{x}}}}{(2\pi)^{N_R} (\sigma_n^2)^{2N_R} M^{2N_T}} \right)}_{\tilde{h}(\mathbf{y})}, \tag{15}$$

where the set of all difference vectors is denoted by

$$\mathcal{D} = \{ \Delta_{\mathbf{x}} \mid \Delta_{\mathbf{x}} = \mathbf{x}_i - \mathbf{x}_\kappa \forall i, \kappa = 1, \dots, N_T^M \}. \tag{16}$$

### 3.2. Approximation

With (15) a rather loose lower bound  $\tilde{h}(\mathbf{y})$  has been formulated, however, the overall behavior is similar to the original entropy. In the limit of very small and very large transmit power  $\mathcal{P}$  (assuming a fixed noise power  $\sigma_n^2 = 1$ ) the difference to the true entropy is constant as the following analysis shows

$$\lim_{\substack{\mathcal{P} \rightarrow \infty \\ \sigma_n^2 = 1}} \tilde{h}(\mathbf{y}) = N_R \log_2(2\pi M^{N_T}) \tag{17}$$

$$\lim_{\substack{\mathcal{P} \rightarrow 0 \\ \sigma_n^2 = 1}} \tilde{h}(\mathbf{y}) = N_R \log_2(2\pi). \tag{18}$$

Where (18) is obvious as all exponential terms in (15) tend to one for  $\mathcal{P} \rightarrow 0$ , whereas (17) results due to the fact that

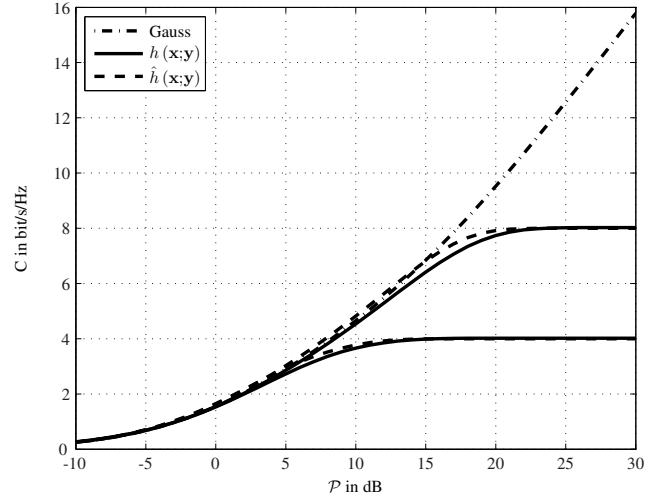


**Fig. 1.** Comparison of  $h(\mathbf{x};\mathbf{y})$  and  $\hat{h}(\mathbf{x};\mathbf{y})$  for a random channel ( $N_R = N_T = 2$ , 4-QAM and 16-QAM)

all exponential terms with  $i \neq \kappa$  tend to zero for  $\mathcal{P} \rightarrow \infty$ . Accordingly, the limits of  $h(\mathbf{y})$  can be calculated

$$\lim_{\substack{\mathcal{P} \rightarrow \infty \\ \sigma_n^2 = 1}} h(\mathbf{y}) = N_R \log_2(\pi e M^{N_T}) \tag{19}$$

$$\lim_{\substack{\mathcal{P} \rightarrow 0 \\ \sigma_n^2 = 1}} h(\mathbf{y}) = N_R \log_2(\pi e) \tag{20}$$

Apparently, the difference  $\Delta_{h(\mathbf{y})}$  between  $h(\mathbf{y})$  and  $\tilde{h}(\mathbf{y})$  for very low or high SNR is given by

$$\Delta_{h(\mathbf{y})} = N_R \log_2\left(\frac{e}{2}\right). \tag{21}$$

Due to this we propose an approximation  $\hat{h}(\mathbf{y})$  to the entropy  $h(\mathbf{y})$  based on Jensen's inequality

$$h(\mathbf{y}) \approx \hat{h}(\mathbf{y}) = \tilde{h}(\mathbf{y}) + \Delta_{h(\mathbf{y})}. \tag{22}$$

Fig. 1 shows the proposed approximation and the exact capacity (via numerical integration) for 4-QAM and 16-QAM.

For comparison, the well known capacity with Gaussian signaling has been plotted. A randomly generated realization of a channel matrix  $\mathbf{H}$  ( $h_{i,\kappa} \sim \mathcal{N}_C(0, 1)$ ) with  $N_R = N_T = 2$  has been used to achieve the results. The general behavior of the channel capacity  $h(\mathbf{x};\mathbf{y})$  is well approximated by  $\hat{h}(\mathbf{y})$  with the biggest deviation in the transient part of the curve. Even though this form is more tractable than  $h(\mathbf{y})$ , it is still numerically demanding for high rates and large systems.

#### 4. CHANNEL DECOMPOSITION

In order to ease calculation of the constrained channel capacity, two decomposition approaches will be investigated. Regarding a Single Input Single Output (SISO) channel the capacity can be approximated based on knowledge of the SNR and some curve fitting [4]. Accordingly, we are interested in a way to represent the MIMO capacity in terms of subchannel SINRs. This way, either the presented approximation (22) or other known solutions can be incorporated to estimate the mutual information.

##### 4.1. Singular Value Decomposition

An often invoked approach considering MIMO systems is the decomposition of the channel matrix  $\mathbf{H}$  to

$$\mathbf{H} = \mathbf{U}\mathbf{S}\mathbf{V}^H, \quad (24)$$

where  $\mathbf{U}$  and  $\mathbf{V}$  are unitary matrices and  $\mathbf{S} = \text{diag}(\lambda_1, \dots, \lambda_r)$  denotes the diagonal matrix of singular values  $\lambda_i$  with  $r$  being the rank of the channel matrix.

Introducing (24) to (1) again neglecting  $k$ , we achieve  $r$  equivalent SISO systems

$$\begin{aligned} \mathbf{y} &= \mathbf{U}\mathbf{S}\mathbf{V}^H\mathbf{x} + \mathbf{n} \quad \text{and} \quad \mathbf{x} = \mathbf{V}\sqrt{\frac{\mathcal{P}}{N_T}}\mathbf{d} \\ \tilde{\mathbf{y}} &= \mathbf{U}^H\mathbf{y} = \mathbf{S}\sqrt{\frac{\mathcal{P}}{N_T}}\mathbf{d} + \tilde{\mathbf{n}} \\ \tilde{y}_i &= \lambda_i\sqrt{\frac{\mathcal{P}}{N_T}}d_i + \tilde{n}_i \quad \forall i = 1, \dots, r. \end{aligned} \quad (25)$$

The  $SNR_i$  of each layer  $i$  can be expressed in terms of the signal to noise ratio  $\mathcal{P}/(N_T\sigma_n^2)$  and the singular values  $\lambda_i$

$$SNR_i = \frac{\mathcal{P}\lambda_i^2}{N_T\sigma_n^2}. \quad (26)$$

Thus, considering Gaussian signaling the capacity can be formulated as a sum of subchannel capacities depending on the singular values  $\lambda_i$  of the channel [11]. With a discrete signal alphabet, however, this is no longer viable, as the decomposition of the channel into orthogonal subchannels leads to a different overall mutual information of the system. Specifically, (4) is transformed into a sum of independent terms resulting in (23).

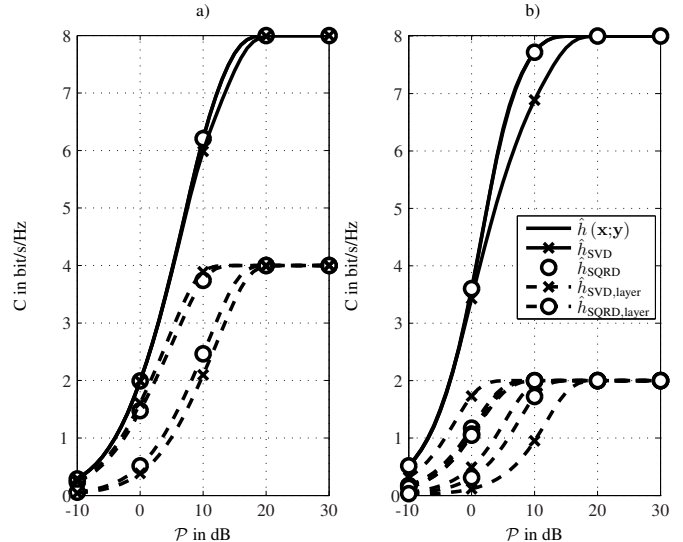


**Fig. 2.** Comparison of the mutual information of SVD and QR based channel decompositions with the mutual information of the system, a)  $N_T = N_R = 2$ ,  $M = 16$ , b)  $N_T = N_R = 4$ ,  $M = 4$

##### 4.2. QR decomposition

Another well known approach to decompose a channel matrix is the SQRD, which enables the decomposition in the sense of the MMSE with sorting of the layers [12]. Introducing the extended channel matrix  $\tilde{\mathbf{H}} = \begin{bmatrix} \mathbf{H}\mathbf{\Omega} \\ \sigma_n\mathbf{I}_{N_T} \end{bmatrix}$  with the permutation matrix  $\mathbf{\Omega}$ , the decomposition is defined as

$$\tilde{\mathbf{H}} = \tilde{\mathbf{Q}}\tilde{\mathbf{R}}, \quad (27)$$

where  $\tilde{\mathbf{Q}}$  is a matrix with orthogonal columns and  $\tilde{\mathbf{R}}$  is upper triangular.

The  $SNR_i$  of each layer  $i$  can be expressed in terms of the signal to noise ratio  $\mathcal{P}/(N_T\sigma_n^2)$  and the diagonal elements of  $\tilde{\mathbf{R}}$

$$SNR_i = |r_{i,i}|^2 \frac{\mathcal{P}}{N_T\sigma_n^2} - 1. \quad (28)$$

An approximate mutual information  $h_{\text{SQRD}}(\mathbf{y})$  can then be attained by replacing  $\lambda_i\sqrt{\mathcal{P}/N_T}$  with  $\sqrt{SNR_i}$  in (23).

##### 4.3. Comparison

Fig. 2 shows a comparison of the channel capacity as defined by the approximation (22) to the corresponding SISO capacities and their sum in case of SVD and QR decomposition of the system, i.e.  $\hat{h}_{\text{SVD}}$  and  $\hat{h}_{\text{SQRD}}$ . Regarding the QR decomposition sub-optimal sorting with MMSE filtering is used [12]. The system parameters for a) are  $N_R = N_T = 2$  with  $M = 16$ . Part b) of Fig. 2 shows results for  $N_R = N_T = 4$  and  $M = 4$ . The chosen channel realizations are

$$h_{\text{SVD}}(\mathbf{y}) = \sum_{i=1}^r \int_{\mathcal{C}} \frac{1}{M^2 2\pi\sigma_n^4} \sum_{d_i \in \mathcal{A}} e^{-|\tilde{y}_i - \lambda_i \sqrt{P/N_T} d_i|^2} \log_2 \left( \frac{1}{M^2 2\pi\sigma_n^4} \sum_{d_i \in \mathcal{A}} e^{-|\tilde{y}_i - \lambda_i \sqrt{P/N_T} d_i|^2} \right) d\tilde{y}_i \quad (23)$$

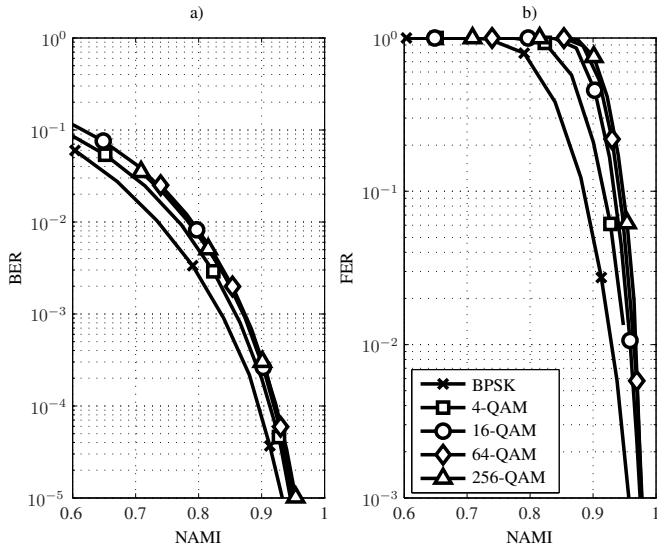


**Fig. 3.** a) Bit Error Rate and b) Frame Error Rate versus normalized Mutual Information,  $N_R = N_T = 2$ ,  $N_C = 1024$  for  $M$ -QAM with  $M = 1, \dots, 8$  - max-APP, Convolutional Code

both "good" in the sense of nearly equally good singular values. Largely different singular values are usually unfavorable for the SVD (without any kind of adaptation), leading to bad approximations. Even in this "good" case, where the difference between the singular values is small, the approximation is clearly worse than for the SQRD approach. All the more if the number of antennas grows, as can be seen in b). Note, that  $\hat{h}_{\text{SQRD}}$  is depicted with markers only since the results are equal to  $\hat{h}(x;y)$ . Both approaches lead to usable approximations (for the shown "good" channels), but the QR approach - a consequence of the sorting - is clearly superior and even performs well if the singular values differ greatly. Therefore, the SQRD approach will be used to ease the calculation of the mutual information by approximation (22) as a sum of SISO terms in the remainder of the paper.

## 5. RATE ALLOCATION

As stated in Section 2 we consider a system, where spatial multiplexing is applied per subcarrier and the available transmit power is allocated evenly to all subcarriers and antennas.

Under these circumstances the used modulation size on each subcarrier shall be adapted to the communication chan-

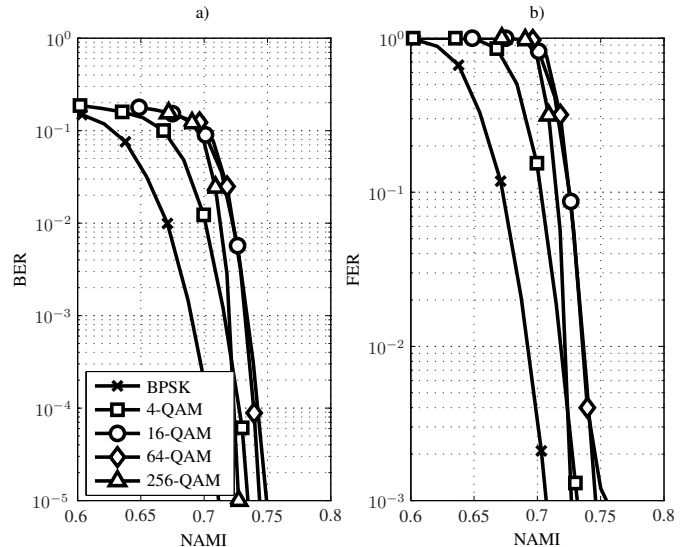


**Fig. 4.** a) Bit Error Rate and b) Frame Error Rate versus normalized Mutual Information,  $N_R = N_T = 2$ ,  $N_C = 1024$  for  $M$ -QAM with  $M = 1, \dots, 8$  - max-APP, Turbo Code

nel assuming perfect channel state information at the transmitter. Note, however, that due to the system assumptions transmitter knowledge of the chosen modulation on a given subcarrier is sufficient, which makes this approach feasible even in feedback constrained scenarios. In order to incorporate channel coding into the design of our rate allocation scheme, we consider the normalized average mutual information (NAMI) of an OFDM symbol

$$\text{NAMI} = \frac{1}{N_C} \sum_{k=1}^{N_C} \frac{\text{MI}(\mathbf{H}_k, \mathcal{A}_k)}{N_T \log_2(M_k)}, \quad (29)$$

where  $\text{MI}(\mathbf{H}_k, \mathcal{A}_k)$  denotes the approximated mutual information of a subcarrier  $k$ , which depends on the current channel condition and the chosen modulation alphabet  $\mathcal{A}_k$  and can be calculated via the SQRD and (22). The overall system behavior including channel coding can then be described in terms of the bit or frame error rate depending on the NAMI.

Fig. 3 and Fig. 4 show the error rates in dependence of the NAMI, which have been achieved by Monte Carlo simulations (i.e., random channel realizations) with the system parameters  $N_R = N_T = 2$ ,  $N_C = 1024$  using the convolutional code and the turbo code with max-APP detection, respectively. For each channel realization the NAMI has been calculated along the errors after decoding assuming  $L_F = 1024$ ,



leading to an average performance measure. As can be seen from Fig. 3 the achieved bit and frame error performance versus the normalized average mutual information is approximately independent from the chosen modulation size under the assumption that the same alphabet has been used for all transmit antennas and subcarriers (this is also true for rectangular QAM alphabets which have been omitted due to space constraints). OFDM frames with mixed modulation alphabets on the subcarriers will naturally behave very similar with regard to the NAMI, which motivates the choice of a common threshold for all alphabet sizes to be estimated as the mean of the individual NAMI thresholds of the applied modulation alphabets. This heuristic provides control over the achieved performance as will be shown in Section 6. Motivated by this observation we propose the algorithm *MaxNAMI*, which chooses the rate of a subcarrier according to its mutual information approximated by (22) to achieve a rate constraint. The choice of a minimum (frame or bit) error rate  $ER_{\min}$  provides an operating point leading to a mutual information threshold (i.e. NAMI) which has to be achieved at every subcarrier.

**MaxNAMI** Set the target rate per subcarrier  $R_{\text{Target}}$ , the target error rate  $ER_{\min}$  and the maximum bits per antenna  $i_{\max}$ . Then determine the minimum mutual information  $MI_{\min} = f(ER_{\min})$  necessary to fulfill the bit error rate requirement (dependent on the code, for example per Fig. 3).

1. Calculate the mutual information  $MI(\mathbf{H}_k, \mathcal{A}_i)$  for all subcarriers  $k = 1, \dots, N_C$  and symbol alphabets  $\mathcal{A}_i$  via (3), where  $i = \log_2(M_i) < i_{\max}$ .
2. For each subcarrier  $k$  choose the largest alphabet  $\mathcal{A}_i$  fulfilling  $MI(\mathbf{H}_k, \mathcal{A}_i) > MI_{\min}$  and set modulation index of a subcarrier  $S_k = i$ .
3. Calculate  $R = \sum_{k=1}^{N_C} S_k$  and compare to  $R_{\text{Target}}$ . Stop, if the target rate has been achieved, otherwise continue with (a) or (b).
  - (a) If  $R < R_{\text{Target}}$  set  $S_k = S_k + 1$  at subcarrier  $k$ , where the difference  $MI(\mathbf{H}_k, \mathcal{A}_{S_k+1}) - MI_{\min}$  is smallest. Goto 3.
  - (b) If  $R > R_{\text{Target}}$  set  $S_k = S_k - 1$  at subcarrier  $k$ , where the difference  $MI(\mathbf{H}_k, \mathcal{A}_{S_k}) - MI_{\min}$  is smallest. Goto 3.

By this approach, however, the minimum bit error rate is just used as an indicator for the NAMI threshold. Though, for low SNR this threshold will in general not be achievable, whereas for higher SNR the NAMI is maximized under the rate constraint by this greedy approach, thereby providing a better overall error rate performance.

As stated in Section 2 we are not only considering a convolutional coded system, but also apply turbo coding. The overall behavior shown in Fig. 4 is similar to the convolutional code, though the differences between modulations are more distinctive. Nonetheless, the heuristic NAMI threshold provides overall good results. In general, the turbo code needs

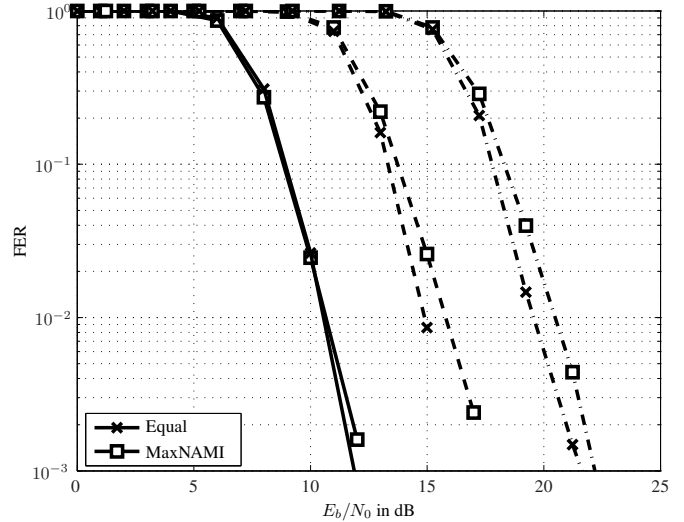


**Fig. 5.** Frame Error Rate versus  $E_b/N_0$ , max-APP detection,  $N_R = N_T = 2$ ,  $N_C = 1024$  and  $L_F = 10$  for 4 Bit/s/Hz (solid), 8 Bit/s/Hz (dashed) and 12 Bit/s/Hz (dash dotted) with  $BER_{\min} = 10^{-3}$  and  $i_{\max} = 8$

much less NAMI per OFDM symbol to achieve reasonable error rates than the convolutional code which is especially attractive for rate optimization under the constraint of a target error rate. Therefore, we propose the algorithm *MinNAMI* as a means to control the NAMI while maximizing the transmission rate.

**MinNAMI** Set the target (bit or frame) error rate  $ER_{\min}$  and the maximum bits per antenna  $i_{\max}$ . Then determine the average mutual information threshold  $NAMI_{\text{Th}} = f(ER_{\min})$  necessary to fulfill the bit error rate requirement (dependent on the code as per Fig. 3 or Fig. 4) and define  $\delta_{\max}$  the maximum tolerated deviation.

1. Calculate the mutual information  $MI(\mathbf{H}_k, \mathcal{A}_i)$  for all subcarriers  $k = 1, \dots, N_C$  and symbol alphabets  $\mathcal{A}_i$  via (3), where  $i = \log_2(M_i) < i_{\max}$ .
2. For each subcarrier  $k$  choose the largest alphabet  $\mathcal{A}_i$  fulfilling  $MI(\mathbf{H}_k, \mathcal{A}_i) > NAMI_{\text{Th}}$  and set  $S_k = i$ .
3. Calculate the current NAMI and compare to  $NAMI_{\text{Th}}$ . Stop, if the target NAMI has been achieved, otherwise continue with 4.
4. If  $NAMI - NAMI_{\text{Th}} > \delta_{\max}$  set  $S_k = S_k + 1$  at subcarrier  $k$ , where the difference  $MI(\mathbf{H}_k, \mathcal{A}_{S_k+1}) - NAMI_{\text{Th}}$  is smallest. Goto 3.

Due to step 2 it is guaranteed, that the current NAMI is always higher or equal to the threshold and due to the fact that the NAMI change at step 4 is always as small as possible with the choice of a reasonable  $\delta_{\max}$  the resulting NAMI will always be higher than the threshold. Because of the hard error

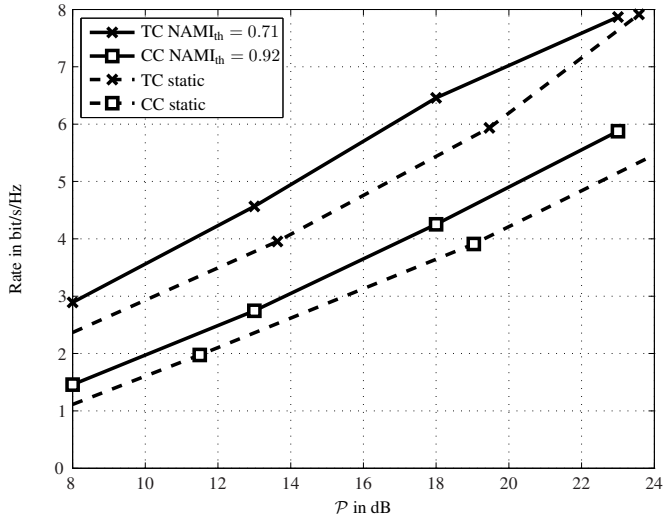


**Fig. 6.** Achieved transmission rate versus  $\mathcal{P}$ , max-APP detection,  $N_R = N_T = 2$ ,  $N_C = 1024$  and  $L_F = 6$  for “Min-NAMI” with  $\text{BER}_{\min} = 10^{-5}$  (CC),  $\text{FER}_{\min} = 10^{-2}$  (TC),  $i_{\max} = 8$  and  $\delta_{\max} = 0.05$ ; Fixed modulation (dashed), Code and  $\text{AMI}_{\text{Th}}$  as noted in the legend (solid)

rate constraint, transmission is not possible for too low transmission powers. Likewise, for high transmission powers the rate will be limited to the highest modulation size leading to a decreasing error rate.

## 6. SIMULATION RESULTS

The following results have been obtained through Monte Carlo simulations using a fixed set of system parameters. Note, that in contrast to the derivations in Section 3 and 4.1 channel matrices are randomly generated for each OFDM symbol.

Regarding *MaxNAMI*, Fig. 5 shows the frame error rate using max-APP detection (a posteriori probability) for a system with  $N_C = 1024$  subcarriers,  $N_R = N_T = 2$  antennas and  $L_F = 10$  channel taps if a rate of 4 Bit/s/Hz, 8 Bit/s/Hz or 12 Bit/s/Hz is transmitted. The results denoted as “Equal” show the performance of a non adaptive system with a fixed modulation alphabet for all subcarriers (4-QAM, 16-QAM and 64-QAM accordingly). The proposed rate allocation scheme, denoted as “MaxNAMI” offers gains of approximately 1dB for 8 Bit/s/Hz and 12 Bit/s/Hz at  $\text{FER} = 10^{-2}$ , where the gain for higher rates increases. This is instantly understandable as more degrees of freedom exist to allocate rate to subcarriers. Accordingly, at 4 Bit/s/Hz noticeable gains occur only below  $\text{FER} = 10^{-2}$ .

In case of Fig. 6 and Fig. 7 a system with  $N_C = 1024$  subcarriers,  $N_R = N_T = 2$  antennas and  $L_F = 6$  channel taps has been used. Fig. 6 presents the achieved transmission rate, which is calculated as the sum of all bits of the error free frames normalized to the number of subcarriers  $N_C$  and the

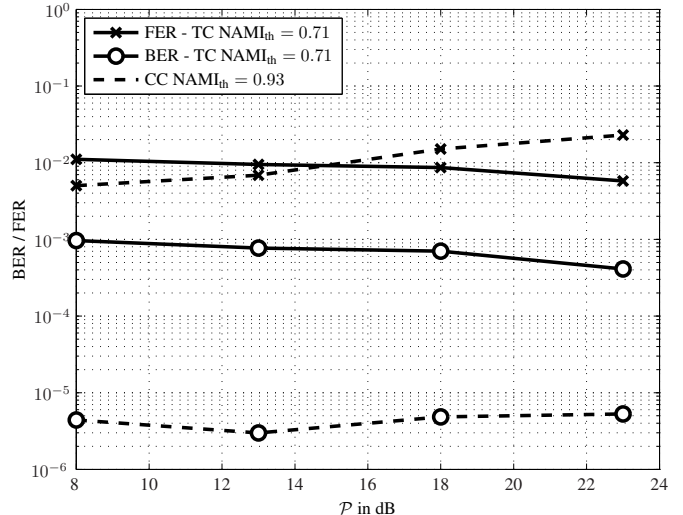


**Fig. 7.** Bit and Frame Error Rate versus  $\mathcal{P}$ , max-APP detection,  $N_R = N_T = 2$ ,  $N_C = 1024$  and  $L_F = 6$  for Algorithm 2 with  $\text{BER}_{\min} = 10^{-5}$  (CC),  $\text{FER}_{\min} = 10^{-2}$  (TC),  $i_{\max} = 8$  and  $\delta_{\max} = 0.05$ ; Derived  $\text{AMI}_{\text{Th}}$  as noted in the legend

number of error free frames. For comparison to the “Min-NAMI” algorithm the maximum achievable rate with respect to a fixed modulation alphabet has been obtained at the given target error rate. With an error rate of  $\text{BER}_{\min} = 10^{-5}$  for the convolutional code and  $\text{FER}_{\min} = 10^{-2}$  for the turbo code the static transmission scheme achieves nearly the maximum possible rate (i.e. 4-QAM achieves 2 bit/s/Hz). Accordingly, the transmission powers for each modulation alphabet have been used as a reference denoted as “static” in Fig. 6. “Min-NAMI” achieves gains of approximately 0.5 bit/s/Hz in case of the convolutional code and up to 1 bit/s/Hz when turbo coding is applied. While the system with turbo coding nearly achieves the maximum possible rate - due to the choice of  $i_{\max} = 8$  (256-QAM) - at  $\mathcal{P} = 23\text{dB}$ , the weak convolutional code is roughly 2 bit/s/Hz inferior. Considering the error rate results in Fig. 7, the target error rates for the turbo code are well met with the exception of  $\mathcal{P} = 23\text{dB}$ , where the proposed scheme already achieves the highest possible rate. For higher transmit powers the error rates will decrease accordingly as only the highest modulation size will be used leading to an increased NAMI as already predicted in Section 4.3. The convolutional code, however, shows an increasing deviation with respect to the chosen threshold, which is especially evident in the frame error rate. The higher the transmit rate, the longer the code words become, which leads to an increasing probability of code word errors. In contrast to the turbo coded system, where longer code words also mean increased interleaver length and therefore a better performance, a fully loaded system performs worse with respect to a given NAMI. Furthermore, at low rates the chosen NAMI threshold is too pessimistic (compare Fig. 3) leading to a decrease-

ing error rate. Due to this, the simple heuristic approach of a common NAMI threshold does not work well for rate optimization with an error constraint when convolutional codes are applied, whereas turbo codes are more robust.

## 7. CONCLUSION

For the specific scenario of a single user OFDM System where spatial multiplexing should be applied and max-APP detection is used, two mutual information based rate allocation schemes have been introduced. Our approach makes use of the inherent connection of capacity and average decoding performance, which still holds for MIMO systems. It has been shown, that through this approach lower BER/FER are achievable via a simple greedy algorithm which maximizes the normalized average mutual information of an OFDM symbol. Secondly, rate optimization given a fixed target BER/FER, which is especially attractive in the presence of ARQ schemes, has been introduced. Here, the simple heuristic threshold calculation only proved to be useful for turbo coded systems, whereas the convolutional code leaves much room for enhancement.

Furthermore, compared to linear schemes which need perfect channel state information at the transmitter based on the SVD of the subcarrier channel matrices, our approach needs less feedback. It is sufficient to signal the transmitter which QAM should be used on a specific subcarrier. The downside, however, is a much higher complexity at the receiver due to the applied max-APP detection. Modern parallel soft output sphere detection [13][14] offers a feasible implementation, but less complex detection at marginal performance losses would be preferable. The application of the SQRD as a means to calculate the capacity of the system naturally leads to another option. Successive Interference Cancellation (SIC) receivers based on the SQRD have been shown to nearly achieve the performance of APP detection at much less complexity.

Future enhancements to these approaches could include the application of multiple thresholds, each tailored to the decoding performance of specific modulation alphabet and/or adaptive thresholds depending on the NAMI currently achievable. The latter seems especially useful to achieve a tight error rate control in case of convolutional codes. Moreover, to overcome the limitation of a maximum alphabet size additionally code rate switching could be included into the design, leading to a mixture of BER/FER vs. NAMI characteristics to choose from.

## 8. REFERENCES

- [1] B.S. Krongold, K. Ramchandran, and D.L. Jones, "Computationally Efficient Optimal Power Allocation Algorithms for Multicarrier Communication Systems," *IEEE Transactions on Communications*, vol. 48, no. 1, pp. 23–27, January 2000.
- [2] R.F.H. Fischer and J.B. Huber, "A New Loading Algorithm for Discrete Multitone Transmission," in *IEEE Global Telecommunications Conference (GLOBECOM)*, London, England, November 1996, pp. 724–728.
- [3] S. Ibi, T. Matsumoto, R. Thom, S. Sampei, and N. Morinaga, "EXIT Chart-Aided Adaptive Coding for Multilevel BICM with Turbo Equalization in Frequency Selective MIMO Channels," *IEEE Transactions on Vehicular Technology*, vol. 56, no. 6, pp. 3757–3769, November 2007.
- [4] H. Sankar and K.R. Narayanan, "Design of Near-Optimal Coding Schemes for Adaptive Modulation with Practical Constraints," in *International Conference on Communications (ICC)*, Istanbul, Turkey, June 2006, vol. 11, pp. 5034–5039.
- [5] Y. Li and W.E. Ryan, "Mutual-Information-Based Adaptive Bit-Loading Algorithms for LDPC-Coded OFDM," *IEEE Transactions on Wireless Communication*, vol. 6, no. 5, pp. 1670–1680, May 2007.
- [6] K. Brueninghaus, D. Astely, T. S'izer, S. Visuri, A. Alexiou, S. Karger, and G. Seraji, "Link performance models for system level simulations of broadband radio access systems," in *IEEE 16th International Symposium on Personal, Indoor and Mobile Radio Communications (PIMRC)*, Berlin, Germany, September 2005, vol. 4, pp. 2306–2311.
- [7] B.M. Hochwald and S. ten Brink, "Achieving Near-Capacity on a Multiple-Antenna Channel," *IEEE Transactions on Communications*, vol. 51, no. 3, pp. 389–399, March 2003.
- [8] A. Ekbal, K. Song, and J.M. Cioffi, "Outage capacity and cut-off rate of bit-interleaved coded OFDM under quasistatic frequency selective fading," in *IEEE Global Telecommunications Conference (GLOBECOM)*, San Francisco, USA, December 2003, vol. 2, pp. 1054–1058.
- [9] H. Zhu, Z. Shi, B. Farhang-Beroujeny, and C. Schlegel, "An Efficient Statistical Approach for Calculation of Capacity of MIMO Channels," in *International Conferences on Wireless and Optical Communications*, Banff, Canada, July 2003.
- [10] 3GPP TSG RAN, "Multiplexing and Channel Coding (FDD)," Tech. Rep. TS 25.212 V7.5.0, May 2007.
- [11] T. Cover and J. Thomas, *Elements of Information Theory*, Wiley & Sons, New York, second edition, 2006.
- [12] D. Wübben, R. Böhnke, V. Kühn, and K.D. Kammeyer, "MMSE Extension of V-BLAST based on Sorted QR Decomposition," in *IEEE Semiannual Vehicular Technology Conference (VTC)*, Orlando, FL, USA, October 2003.
- [13] J. Jalden and B. Ottersten, "Parallel Implementation of a Soft Output Sphere Decoder," in *Asilomar Conference on Signals, Systems and Computers*, Asilomar, CA, USA, November 2005, pp. 1013–1016.
- [14] C. Studer, A. Burg, and H. Bölcskei, "Soft-output sphere decoding: Algorithms and VLSI implementation," *IEEE Journal on Selected Areas in Communications (submitted)*, April 2007.